A high-resolution study of resonant Auger decay processes in N_2O after core electron excitation from terminal nitrogen, central nitrogen and oxygen atoms to the 3π LUMO

2007 J. Phys. B: At. Mol. Opt. Phys. 40 3357

(http://iopscience.iop.org/0953-4075/40/17/004)

IOP Publishing Journal of Physics B: Atomic, Molecular and Optical Physics

J. Phys. B: At. Mol. Opt. Phys. **40** (2007) 3357–3365 doi:10.1088/0953-4075/40/17/004

A high-resolution study of resonant Auger decay processes in N_2O after core electron excitation from terminal nitrogen, central nitrogen and oxygen atoms to the 3π LUMO

M N Piancastelli[1], D Céolin[1], O Travnikova[1], Z Bao[1], M Hoshino[2], T Tanaka[2], H Kato[2], H Tanaka[2], J R Harries[3], Y Tamenori[3], G Prümper[4], T Lischke[4], X J Liu[4] and K Ueda[4]

[1] Physics Department, Uppsala University, PO Box 530, 751 21 Uppsala, Sweden
[2] Department of Physics, Sophia University, Tokyo 102-8554, Japan
[3] Japan Synchrotron Radiation Research Institute, Sayo-gun, Hyogo 679-5198, Japan
[4] Institute of Multidisciplinary Research for Advanced Materials, Tohoku University, Sendai 980-8577, Japan

Received 6 June 2007, in final form 12 July 2007
Published 15 August 2007
Online at stacks.iop.org/JPhysB/40/3357

Abstract

Decay spectra of N_2O following excitation to the N terminal (N_t) $\rightarrow \pi^*$, N central (N_c) $\rightarrow \pi^*$ and O 1s $\rightarrow \pi^*$ intermediate states are reported. The final states reached after participator decay show resonant enhancement consistent with a local-density-of-states analysis based on the Mulliken population of the valence molecular orbitals. In particular, the X-state is resonantly enhanced mostly after excitation from the N_t 1s and the O 1s core levels to the π^*, while the B-state is mostly enhanced following the excitation of the N_c 1s $\rightarrow \pi^*$ intermediate state. Below the N_t 1s threshold, the lowest lying peak related to spectator decay falls at lower binding energy than the highest lying participator peak. This can be attributed to a particularly strong screening effect exerted by the excited electron in the LUMO.

(Some figures in this article are in colour only in the electronic version)

Introduction

The linear triatomic molecule N_2O has attracted a lot of attention due to its peculiar electronic structure, being a very simple example of a triatomic molecule with three light atoms in different chemical environments. Furthermore, the two nitrogen atoms in N_2O are not chemically equivalent, in contrast to the chemically equivalent oxygen atoms in CO_2, a similar linear system. Therefore, it is possible to selectively excite core electrons from either of the nitrogen atoms and observe the differences in the decay processes. Some of the interesting

properties of the two nitrogen atoms with different electron densities are the chemical shift between their ionization energies that one can measure in XPS (about 4 eV) [1–4], where the terminal nitrogen 1s core level exhibits a binding energy of 408.44 eV and the central nitrogen (directly bound to oxygen) has a binding energy of 412.46 eV. As a consequence, there are two overlapping series in normal Auger decay [5, 6]. Furthermore, the energy separation in absorption measurements for transitions from either of the N 1s levels to the same intermediate state is again about 4 eV [7–10]. Some related dynamical properties are the different decay processes one can observe by looking at relaxation phenomena such as resonant Auger decay [11, 12], fragmentation patterns [13–20], etc, which take place after excitation from either of the two N 1s core levels to the same reachable intermediate state. Although the excitation step involving core orbitals is atomic site-selective, the decay-fragmentation processes involve valence states, and therefore one of the interesting points in studying this molecule is to verify if and to what extent the excitation from specific atomic sites affects the subsequent evolution of the system, for example in selectivity in bond breaking according to the atomic site of the primary excitation, or in selective resonant enhancement of spectral features related to the final states reached after resonant Auger decay.

Resonant Auger decay spectra with moderate energy resolution following the two N 1s $\rightarrow$ π^* excitations and the O 1s $\rightarrow$ π^* excitation have been reported some time ago [11]. More recently, results have been reported mainly on the decay properties of the terminal N 1s $\rightarrow$ π^* core-excited state, in particular, concerning the effect of the Renner–Teller splitting in the intermediate state on the nuclear motion detected in the final states reached after participator decay [12]. However, no complete resonant Auger spectra obtained with the state-of-the-art resolution and including all features related to participator and spectator processes in the 10–35 eV binding energy range have yet been published.

We report here a study of the decay spectra of N_2O following the excitation to the N terminal (N_t) $\rightarrow$ π^*, N central (N_c) $\rightarrow$ π^* and O 1s $\rightarrow$ π^* intermediate states. A detailed vibrationally resolved analysis of the effect of the Renner–Teller splitting on the X-state reached after participator decay will be the subject of a separate publication [21]. Here, we concentrate on overview spectra recorded at photon energy values corresponding in all three cases to the top of the resonance and detuning towards the low-energy and the high-energy side. The effect of detuning has been described in several publications [22–24], and in the present case it has allowed us to select some different groups of vibrational states in the intermediate state and to verify how this difference reflects in the final states. In particular, this procedure allows one to study the interplay of the potential curves of the intermediate and the final state in determining the lineshape and the apparent dispersion relationship as a function of excitation energy in the final state.

We observe that the contribution in terms of Mulliken population of the valence molecular orbitals has a crucial role in determining the decay properties of the resonances connected to the three different core levels [25]. In particular, in what concerns the behaviour of the spectral features related to participator decay, the X-state is resonantly enhanced mostly after excitation from the N_t 1s and the O 1s core levels to the π^*, while the A-state shows very little resonant enhancement, and the B-state is mostly enhanced following the excitation of the N_c 1s $\rightarrow$ π^* intermediate state. This behaviour reflects the contribution of the atomic orbitals of the three atoms to the valence electronic density: the X-state ($2\pi^{-1}$) is mostly localized on the terminal nitrogen and the oxygen atoms, while the B-state ($1\pi^{-1}$) is based mainly on the contribution from the central nitrogen atom. In a separate paper [26], we will discuss the direct correlation between these electron density considerations and the fragmentation patterns following the core excitation as observed using electron–ion coincidence techniques.

We also note that the B-state shows a completely different vibrational substructure when reached by direct photoemission or after participator decay: the potential curves of the intermediate state and of the B-state are almost parallel, as can be deduced from the apparent non-dispersion of the related spectral feature as a function of photon energy around the N_c 1s threshold, which is due to vibrational effects.

As for spectator decay, a strong enhancement of spectral features in the same binding energy region as the C-state is visible in both the decay of the N_t 1s $\rightarrow \pi^*$ and of the O 1s $\rightarrow \pi^*$ resonances, although at different binding energies (lower binding energy following the decay of the two N 1s core-excited states and higher binding energy following the decay of the O 1s core-excited state). Following the literature assignment, the lowest lying spectator-related features can be connected to two of the $^2\Pi$ states with $2\pi^{-2}3\pi$ configuration [27]. The non-dispersive behaviour of these peaks again hints at parallel potential curves for the intermediate and final states. Rather interestingly, their relative intensity is very different at the two edges: the lowest lying feature is mostly enhanced following the decay of the N_t 1s $\rightarrow \pi^*$, while the higher binding-energy peak is mostly enhanced following the decay of the O 1s $\rightarrow \pi^*$ resonance. This difference is not simply connected to either atomic population or geometry and remains at the moment unexplained.

Moreover, the energy position for the lowest lying of these two spectral structures for decay processes below the N_t 1s threshold is quite unusual, since the peak falls at lower binding energy than the highest lying participator peak. This can be attributed to a particularly strong screening effect exerted by the excited electron in the lowest unoccupied molecular orbital (LUMO).

Experimental details

The experiment was carried out on the c branch of the soft-x-ray photochemistry beam line 27SU at SPring-8 in Japan [28]. The radiation source is a figure 8 undulator and provides linearly polarized light: the polarization vector E is horizontal for the first-order harmonic light and vertical for the 0.5-order harmonic light [29]. The monochromator installed on this branch is of Hettrick type [30] and provides monochromatic soft x-rays with a bandwidth of $\approx$50 meV in the O 1s excitation region.

The high-resolution electron spectroscopy system employed consists of an SES-2002 hemispherical electron energy analyser, a gas cell and a differentially pumped main chamber [31]. The lens axis of the analyser is in the horizontal direction, and the entrance slit of the analyser is set parallel to the photon beam direction.

Results and discussion

The electron configuration in the ground state of N_2O is as follows:

$$1\sigma^2 2\sigma^2 3\sigma^2 4\sigma^2 5\sigma^2 6\sigma^2 1\pi^4 7\sigma^2 2\pi^4 3\pi,$$

where the deepest lying core orbitals are localized on the oxygen atom (1σ at binding energy 541.2 eV), the central nitrogen atom (2σ at 412.46 eV) and the terminal nitrogen atom (3σ at 408.44 eV) [3]. The inner-valence orbitals 4σ and 5σ, where many-body effects have been demonstrated to be important [32, 33], lie at binding energies of 35.5 and 38.0 eV, respectively. As for the outer-valence orbitals, the 6σ orbital at 20.11 eV has mainly σ_{N-O} bonding character, the 1π orbital at 17.65 eV has a substantial contribution from the central nitrogen atom with a smaller contribution from the oxygen atomic valence orbitals, the 7σ at 16.38 eV is mainly σ_{N-N} in character, and the 2π orbital at 12.89 eV is mainly localized on the terminal nitrogen

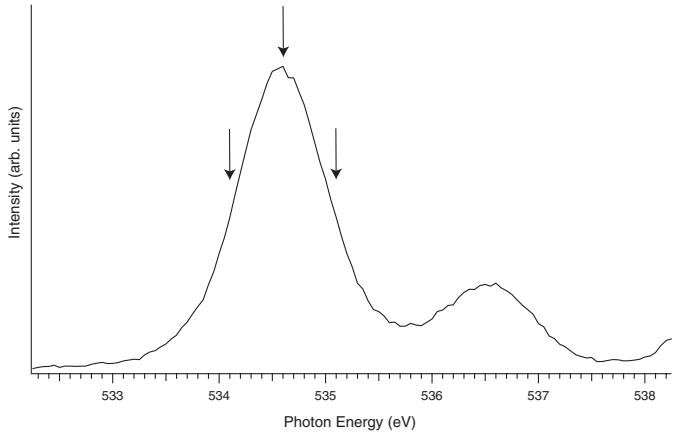

Figure 1. Absorption spectrum obtained in the total ion yield mode below the O 1s ionization threshold. The most intense lowest lying feature corresponds to the O 1s $\rightarrow \pi^*$ transition. The arrows mark the photon energy values where decay spectra were recorded.

and the oxygen atoms [5, 32–34]. The lowest lying empty molecular orbital 3π is distributed almost equally over three atomic sites. We will describe in the following discussion how these localization properties affect the resonant Auger decay processes.

We have recorded resonant Auger decay spectra following the excitation of the N terminal (N_t) 1s $\rightarrow \pi^*$, N central (N_c) 1s $\rightarrow \pi^*$ and O 1s $\rightarrow \pi^*$ intermediate states. In all three cases, decay spectra were recorded in the binding energy region 10–35 eV for three photon energy values corresponding to the top of the resonant feature in the absorption curve, the low-energy side and the high-energy side. The technique of detuning from the top of a resonant structure has been demonstrated to be very informative if one performs experiments under so-called Auger resonant Raman conditions, namely if the total energy resolution (photon + electron kinetic energy) is better than the lifetime broadening of the core-excited state [35]. However, in our case it is not possible to obtain several decay spectra within the linewidth of a single spectral component in the intermediate state, since there is a low-frequency vibrational mode (the bending mode) which has a spacing narrower than the lifetime broadening both below the N K-edges and the O K-edges. Therefore, we use the detuning not to run under Auger Raman conditions, but to sample different portions of the vibrational envelope in the intermediate state and to examine how this difference is reflected in the decay properties and the lineshape of the final-state spectral features. In figure 1, we show an example of such a procedure for the O 1s $\rightarrow \pi^*$ excitation, and we have obtained similar absorption spectra for the other core levels. In the figure, the photon energy values at which the resonant Auger decay spectra were recorded are marked. The photon energy calibration is based on the values from [36].

In figure 2, we show the resonant Auger spectra recorded at photon energies of 401.1 eV (top), 400.7 eV and 401.55 eV around the terminal nitrogen (N_t) 1s $\rightarrow \pi^*$ transition. An off-resonance spectrum measured at 402.8 eV is also shown for comparison. The binding energy scale has been calibrated according to [34]. We will limit our discussion to the binding energy region 12–21 eV, since the spectral features at higher binding energy correspond to several overlapping states related to spectator decay.

We note a pronounced resonant enhancement for the X-state, with subsequent large variation in the accompanying vibrational substructure. In particular, as previously observed [12], when dealing with long-lived intermediate states, excitation of high vibrational overtones can give rise to an intensity enhancement at the location corresponding to the classical turning

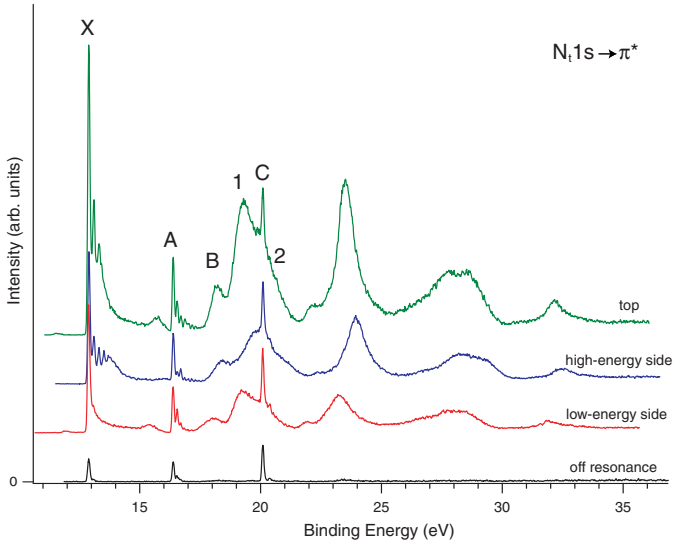

Figure 2. Decay spectra recorded in the photon energy region of the terminal nitrogen (N_t) $1s \rightarrow \pi^*$ transition. The spectra were recorded at 401.1 eV (top), 400.7 eV (low-energy side) and 401.55 eV (high-energy side). An off-resonance spectrum recorded at 402.8 eV is shown for comparison.

points (inner and outer) of the intermediate state's potential energy curve. We interpret the broad maximum around 15.7 eV as a projection of the vibrational wavefunction at the outer classical turning point.

We note a less-pronounced increase in intensity for the A and (even less) for the B states. In the binding energy region of the C-state, we observe a strong resonant enhancement, which is interestingly not attributable to the C-state, which shows a relatively small effect, but rather to another broad and partly overlapped spectral structure upon which the sharp feature related to the C-state is superimposed. This broad feature, labelled 1 in figure 2, shows a non-dispersive behaviour which is informative on the interplay between the potential curves of the intermediate and the final states. Namely, it apparently changes binding energy as a function of photon energy. We have observed such behaviour in several cases, and for broad structures not attributable to ultrafast dissociation processes it has been explained by the fact that the potential curves of the intermediate and of the final states are parallel. Therefore, when by changing photon energy a different group of vibrational states is selected in the intermediate state, the same group is selected in the final state, and the apparent change in binding energy is actually a change in vibrational distribution.

Along with this behaviour, another interesting point for the broad structure is its binding energy position (19.59 eV). Even taking into account the apparent shift of the peak, we note that its binding energy is lower than the binding energy of the C-state. This peak has been assigned upon calculations based on the SAC-CI general-*R* method. The electron configuration for this state is the same as the lowest lying two-hole state reached after normal Auger decay, which is $2\pi^{-2}$, plus an electron in the LUMO (3π orbital) [27]. Therefore, we attribute it to the lowest lying state reached after spectator decay. Usually, spectator states lie at higher binding energies than participator states, but possibly in the present case we can explain the effect with a stronger than usual screening effect of the electron which remains in the state reached by the primary excitation. We note that the same state is visible in the decay spectra recorded

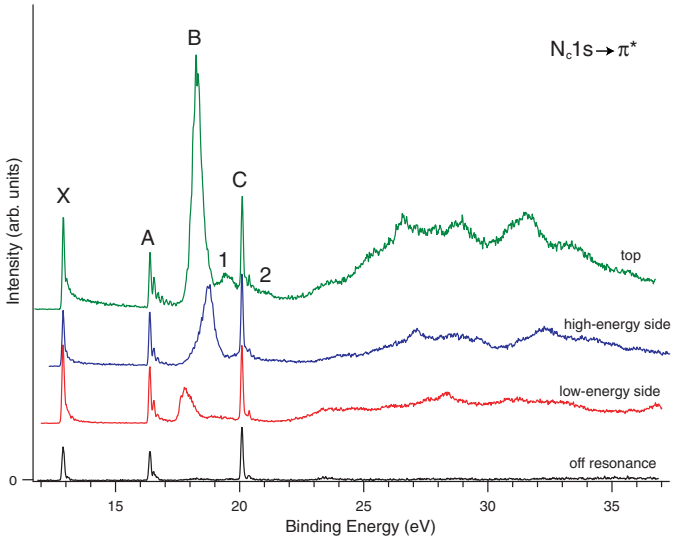

Figure 3. Decay spectra recorded in the photon energy region of the central nitrogen (N_c) 1s $\rightarrow$ π^* transition. The spectra were recorded at 404.7 eV (top), 403.95 eV (low-energy side) and 405.25 eV (high-energy side). An off-resonance spectrum recorded at 402.8 eV is shown for comparison.

after the nitrogen central (N_c) 1s $\rightarrow$ π^* excitation (see the discussion below), although with lower intensity, which is consistent with the weaker coupling of this state with the $2\pi^{-2}3\pi$ state than other core-excited intermediate states. The following structure at 20.94 eV, labelled 2, is barely visible after the decay of the (N_t) 1s $\rightarrow$ π^* core-excited state and will be discussed in detail later.

In figure 3, we show the decay spectra recorded in the photon energy region of the (N_c) 1s $\rightarrow$ π^* resonance. The spectra were recorded at photon energies of 404.7 eV (top), 403.95 eV (low-energy side) and 405.25 eV (high-energy side). An off-resonance spectrum measured at 402.8 eV is also shown for comparison. The spectra exhibit marked differences with those recorded at the (N_t) 1s $\rightarrow$ π^* resonance shown in figure 2. In particular, the relative intensity of the participator-related features reflects the contribution of the central nitrogen to the valence orbitals. We note a relatively weak enhancement of the X, A and C states, while the B-state shows a substantially enhanced intensity. This can be explained on the ground of a larger contribution of the central nitrogen atomic orbitals to the B-state. Furthermore, we observe the non-dispersive behaviour of this feature, and we conclude, in analogy with the similar behaviour described above, that the potential curves of the intermediate state and the B final state are parallel.

In figure 4, we show the decay spectra recorded in the photon energy region of the O 1s $\rightarrow$ π^*excitation. The spectra were recorded at photon energies of 534.6 eV (top), 534.1 eV (low-energy side) and 535.1 eV (high-energy side). An off-resonance spectrum recorded at 532.25 eV is also shown for comparison. A first observation is that the region including features related to spectator decay has a higher relative intensity compared to features related to participator decay in the O 1s decay than in both the N_t and N_c decay. This is a general behaviour, and it is related to the depth of the core hole induced by the primary excitation: the deeper the core hole (in this case O 1s versus N 1s), the more likely it is for the excited electron to remain in the previously empty orbital and not to participate in the decay (see, e.g., [37]).

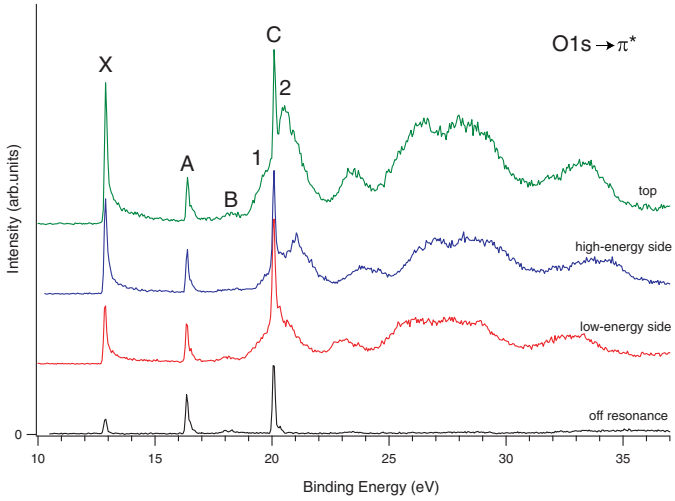

Figure 4. Decay spectra recorded in the photon energy region of the O 1s $\rightarrow \pi^*$ transition. The spectra were recorded at 534.6 eV (top), 534.1 eV (low-energy side) and 535.1 eV (high-energy side). An off-resonance spectrum recorded at 532.25 eV is shown for comparison.

Table 1. N_t 2p and O 2p populations of the two $^2\Pi$ states with $2\pi^{-2}3\pi$ configurations and binding energies of 19.59 and 20.94 eV in comparison with other states, for three different geometries, obtained from SAC-CI calculations including up to triple excitations using a double zeta basis set [38].

			Population	
State	IP (eV)	Intensity	N_t(2p)	O(2p)
Equilibrium linear structure ($R_{NN} = 1.128$ Å, $R_{NO} = 1.184$ Å, angle $= 180°$)				
X	12.46	0.86	2.73	3.82
B	18.23	0.48	2.83	3.83
$^2\Pi$	19.59	0.22	2.75	3.78
$^2\Pi$	20.18	0.00	2.73	3.72
$^2\Pi$	20.94	0.01	2.73	3.74
Bent structure ($R_{NN} = 1.128$ Å, $R_{NO} = 1.184$ Å, angle $= 170°$)				
X	12.34	0.86	2.73	3.81
B	18.12	0.46	2.83	3.82
$^2\Pi$	19.36	0.23	2.76	3.78
$^2\Pi$	19.97	0.00	2.73	3.72
$^2\Pi$	20.81	0.01	2.74	3.74
NO-elongated structure ($R_{NN} = 1.128$ Å, $R_{NO} = 1.25$ Å, angle $= 180°$)				
X	12.36	0.86	2.73	3.78
B	17.93	0.55	2.82	3.84
$^2\Pi$	19.45	0.16	2.74	3.73
$^2\Pi$	20.14	0.00	2.73	3.68
$^2\Pi$	20.88	0.01	2.73	3.71

We note some resonant enhancement for the X-state, since the O atomic orbitals have a high contribution to this valence level. The resonant enhancement of the A, B and C states is negligible. The energy position of the lowest lying visible feature related to spectator decay

(20.94 eV), labelled 2 in figure 3, is different from the position of the lowest lying spectator-related peak observed following the decay of the two N 1s $\rightarrow \pi^*$ excitations (19.59 eV) (feature 1), which hints at a different nature for the final state. Therefore, we assign it as the third $^2\Pi$ state with $2\pi^{-2}3\pi$ configuration (the second one is calculated to have zero intensity) [27]. It is interesting to observe that the two observable peaks related to spectator processes leading to $^2\Pi$ states with the same $2\pi^{-2}3\pi$ configuration exhibit very different relative intensities in the decay spectra following the $(N_t) \rightarrow \pi^*$ and the O 1s $\rightarrow \pi^*$ excitations. Preliminary calculations have ruled out the possibility of such a difference being due to different atomic populations or different geometries. In table 1, we report the N_t 2p and O 2p populations of these two states in comparison with some of the outer valence states [38]. These populations do not change significantly in comparison with other states. The situation is nearly the same even if the molecule is bent or the NO bond length is elongated. Therefore, we cannot link the observed difference in relative intensity to a change in atomic population or a change in geometry. Theoretical investigations are in progress in order to gain a deeper insight into this particular issue.

Conclusion

We have studied the decay spectra of N_2O following excitation to the N terminal $(N_t) \rightarrow \pi^*$, N central $(N_c) \rightarrow \pi^*$ and O 1s $\rightarrow \pi^*$ intermediate states. The contribution in terms of Mulliken population of the valence molecular orbitals determines the decay properties of the resonances connected to the three different core levels. In particular, the X-state is resonantly enhanced mostly after excitation from the N_t 1s and the O 1s core levels to the π^*, and the B-state is mostly enhanced following the excitation of the N_c 1s $\rightarrow \pi^*$ intermediate state. The B-state shows a completely different vibrational substructure when reached by direct photoemission or after participator decay: the potential curves of the intermediate state and of the B-state are almost parallel, as can be deduced from the apparent non-dispersion of the related spectral feature as a function of photon energy around the N_c 1s threshold, which is due to vibrational effects.

As for spectator decay, a strong enhancement of spectral features in the same binding energy region as the C-state is visible in the decays of both the N_t 1s $\rightarrow \pi^*$ and the O 1s $\rightarrow \pi^*$ resonances. Although the two lowest lying peaks are assigned to the same electron configuration, their relative intensity is very different at the different edges. Preliminary calculations have ruled out both differing atomic populations and a change in geometry. Further theoretical calculations are under way to clarify this specific point.

Acknowledgments

We wish to thank M Ehara and O Takahashi for sharing with us the results of their theoretical calculations prior to publication. This experiment was carried out with the approval of the SPring-8 program advisory committee and supported in part by grants-in-aid for Scientific Research from the Japan Society for the Promotion of Science and by the Matsuo Foundation. We are grateful to the staff at SPring-8 for their help.

References

[1] Siegbahn K, Nordling C, Johansson G, Hedman J, Heden P F, Hamrin K, Gelius U, Bergmark T, Werme L O, Manne R and Baer Y 1969 *ESCA Applied to Free Molecules* (Amsterdam: North-Holland)

[2] Schmidbauer M, Kilcoyne A L D, Randall K J, Feldhaus J and Bradshaw A M 1991 *J. Chem. Phys.* **94** 5299

[3] Alagia M *et al* 2005 *Phys. Rev.* A **71** 012506
[4] Ehara M *et al* 2007 *Chem. Phys. Lett.* **438** 14
[5] Larkins F P 1987 *J. Chem. Phys.* **86** 3239
[6] Bolognesi P, Coreno M, Avaldi L, Storchi L and Tarantelli F 2006 *J. Chem. Phys.* **125** 054306
[7] Wright G R and Brion C E 1974 *J. Electron Spectrosc. Relat. Phenom.* **3** 191
[8] Bianconi A, Petersen H, Brown F C and Bachrach R Z 1978 *Phys. Rev.* A **17** 1907
[9] Adachi J, Kosugi N, Shigemasa E and Yagishita A 1995 *J. Chem. Phys.* **102** 7369
[10] Tanaka T *et al* 2006 *Chem. Phys. Lett.* **428** 34
[11] Larkins F P, Eberhardt W, Lyo I-W, Murphy R and Plummer E W 1988 *J. Chem. Phys.* **88** 2948
[12] Miron C *et al* 2001 *J. Chem. Phys.* **115** 864
[13] Murakami J, Nelson M C, Anderson S L and Hanson D M 1986 *J. Chem. Phys.* **85** 5755
[14] Murphy R and Eberhardt W 1988 *J. Chem. Phys.* **89** 4054
[15] Ferrand-Tanaka L, Simon M, Thissen R, Lavollée M and Morin P 1996 *Rev. Sci. Instrum.* **67** 358
[16] LeBrun T, Lavollée M, Simon M and Morin P 1993 *J. Chem. Phys.* **98** 2534
[17] Bozek J D, Saito N and Suzuki I H 1993 *J. Chem. Phys.* **98** 4652
[18] Lee K, Hulbert S L, Kuiper P, Ji D and Hanson D M 1994 *Nucl. Instrum. Methods* A **34** 446
[19] Chen S-Y, Ma C-I, Hanson D M, Lee K and Kim D Y 1998 *J. Electron Spectrosc. Relat. Phenom.* **93** 61
[20] Machida M, Lavollée M, Randrianjafisoa J, Laurent G, Nagoshi M, Okada K, Koyano I and Saito N 2004 *J. Chem. Phys.* **120** 3635
[21] Travnikova O *et al*, to be published
[22] Gel'mukhanov F and Ågren H 1996 *Phys. Rev.* A **54** 379
[23] Sundin S, Kh Gel'mukhanov F, Ågren H, Osborne S J, Kikas A, Björneholm O, Ausmees A and Svensson S 1997 *Phys. Rev. Lett.* **79** 1451 and references therein
[24] Björneholm O, Sundin S, Svensson S, Marinho R R T, Naves de Brito A, Gel'mukhanov F and Ågren H 1997 *Phys. Rev. Lett.* **79** 3150
[25] Cini M, Maracci F and Platania R 1986 As for the use of Mulliken population analysis in Auger spectroscopy see, e.g., *J. Electron. Spectrosc. Relat. Phenom.* **41** 37
[26] Céolin D *et al*, to be published
[27] Ehara M, Yasuda S and Nakatsuji H 2003 *Z. Phys. Chem.* **217** 161 and references therein
[28] Ohashi H, Ishiguro E, Tamenori Y, Kishimoto H, Tanaka M, Irie M and Ishikawa T 2001 *Nucl. Instrum. Methods* A **467** 529
[29] Tanaka T and Kitamura H 1996 *J. Synchrotron Radiat.* **3** 47
[30] Ohashi H *et al* 2001 *Nucl. Instrum. Methods* A **468** 533
[31] Shimizu Y *et al* 2001 *J. Electron. Spectrosc. Relat. Phenom.* **63** 114–6
[32] Domcke W, Cederbaum L S, Schirmer J, Von Niessen W, Brion C E and Tan K H 1979 *Chem. Phys.* **40** 171
[33] Holland D M P, MacDonald M A and Hayes M A 1990 *Chem. Phys.* **142** 291
[34] Kimura K, Katsumata S, Achiba Y, Yamaxaki T and Iwata S 1981 *Handbook of He1 Photoelectron Spectra of Fundamental Organic Molecules* (New York: Halsted)
[35] Kivimäki A, Naves de Brito A, Aksela S, Aksela H, Ausmees A, Osborne S, Dantas L B and Svensson S 1993 *Phys. Rev. Lett.* **71** 4307
[36] Tanaka T *et al* 2007 *Chem. Phys. Lett.* **435** 182
[37] Piancastelli M N, Neeb M, Kivimäki A, Kempgens B, Köppe H M, Maier K, Bradshaw A M and Fink R F 1997 *J. Phys. B: At. Mol. Opt. Phys.* **30** 5677
[38] Ehara M 2007 Private Communication